HIGH FREQUENCY ASYMPTOTICS, HOMOGENIZATION AND LOCALIZATION FOR LATTICES

by R. V. Craster[1,3], J. Kaplunov[2] and J. Postnova[3]

([1] *Department of Mathematical and Statistical Sciences, University of Alberta, Edmonton, T6G 2G1, Canada.*
[2] *Department of Mathematical Sciences, Brunel University, Uxbridge, Middlesex, UB8 3PH, U.K.*
[3] *Department of Mathematics, Imperial College London, South Kensington, London, SW7 2AZ, U.K.*)

[Received December 9, 2010]

Summary

A two-scales approach, for discrete lattice structures, is developed that uses microscale information to find asymptotic homogenized continuum equations valid on the macroscale. The development recognises the importance of standing waves across an elementary cell of the lattice, on the microscale, and perturbs around the, potentially high frequency, standing wave solutions. For examples of infinite perfect periodic and doubly-periodic lattices the resulting asymptotic equations accurately reproduce the behaviour of all branches of the Bloch spectrum near each of the edges of the Brillouin zone. Lattices in which properties vary slowly upon the macroscale are also considered and the asymptotic technique identifies localised modes that are then compared with numerical simulations.

1. Introduction

Discrete mass-spring lattice systems form classical models of crystal vibrations in solid state physics (**1**, **2**) and were used by Newton, Kelvin, Born, and many others, to model and interpret wave phenomena and these models were instrumental in the development of wave mechanics; a review of the historical literature is contained in Brillouin's monograph (**2**). Lattice models remain a valuable and instructive way of modelling and understanding fundamental wave phenomena in crystal lattices and cellular structures (**3**). A common characteristic behaviour of such models is that they exhibit band-gaps, (**4**), namely bands of frequencies for which waves do not propagate through the atomic lattice. More recently such discrete models have been used for engineering structures (**5**) with a view to designing smart structures capable of filtering out various frequencies. These discrete systems, exhibiting band gap behaviour, are closely related to periodic continuous media, for instance photonic crystal fibres (**6**, **7**, **8**), for which band-gaps occur and that have numerous and varied industrial applications; in some limits there is a direct analogy between the discrete and continuum models (**9**). In the mechanics of cellular structures and lattices, considerable knowledge has been gained about the static and low-frequency behaviour in terms of homogenized models, but comparatively less is known of their high frequency behaviour.

A common feature of both discrete and continuum models, that are defect-free and infinite in extent, is that the periodicity of the structure leads to dispersion relations between

frequency and Bloch wavenumber; the latter being the phase shift that a wave exhibits as it passes through one of the periodic cells that form the structure. The periodic cell structure means that there are only a finite range of Bloch wavenumbers that are of interest and these form the irreducible Brillouin zone and within, and at the edges of, this zone there are critical wavenumbers for which standing waves occur; these standing waves can occur at high frequencies. The behaviour of the solutions near these standing wave frequencies is often associated with the extrema of the range of stop-band frequencies, although there are counter-examples where the extrema occur within the Brillouin zone (**10**). The fact that pass- and stop-band behaviour is apparent for such structures suggests their use as mechanical frequency and spatial filters (**5**, **11**). Our aim is to develop asymptotic techniques capable of describing the solutions near frequencies that allow for standing waves; these are potentially high frequencies. The methodology generates continuum partial differential equations (PDEs) that have the micro-structural behaviour in-built. In part, our interest is also in the localised defect modes can occur if the crystal lattice or cellular structure is imperfect (**12**) and one by-product of the asymptotic scheme that we develop is that the high frequency homogenization model captures localization effects. This approach is complementary to recent work on defect states using band gap Green's functions (e.g. for lattices (**13**) and in photonics (**14**, **15**)); the asymptotics of the Green's function and localized defect modes near the edges of the Brillouin zone are related, at least conceptually, to the homogenization model. Green's functions for lattices are of interest in their own right, and have a long history, see (**16**) and the references therein.

In the continuous case the authors (**17**) have developed an asymptotic scheme based upon a separation of scales and demonstrated the efficacy of high frequency homogenized models, that consist of an equation entirely on the macro-scale, but incorporating integrated quantities over the microscale, in modelling wave phenomena on the macroscale. We now turn our attention to the discrete analogue and show that these too can be analysed using a two-scales approach; there are two disparate lengthscales in the system, that of a local periodic cell (the elementary cell) and that of the global structure itself. The essential insight is that, for critical frequencies, standing waves form across the elementary cells that form the medium; in terms of the Bloch wavenumber these are high frequency "long waves" and so can be analysed in a similar manner to the high frequency long waves that occur near transverse thickness resonance in waveguides (**18**, **19**, **20**) for which localised solutions can also be found (**21**, **22**). It is worth noting that the idea of long waves in crystal acoustics and solid state physics is usually limited to the lowest acoustical phonon branch that passes through the origin in frequency-wavenumber space, but that the ideas we develop are valid at high frequency and for standing waves formed at the edges of the Brillouin zone; they can correspond to in-phase or out-of-phase motion of the masses across an elementary cell on the microscale.

The plan of this paper is as follows: we begin, in section 2, by illustrating our ideas on the classical diatomic chain (**2**) with a slight variation in that the masses of each type are not necessarily constant, but can vary with position. One useful check upon the analysis, and illustrative example, is that of Bloch waves for an infinite chain and we explicitly return to this example throughout the text; for the diatomic chain it is dealt with in section 2.2. Bloch waves require each type of mass to remain constant, allowing the masses to vary can lead to localised modes and these are found both directly from the full equations and from the asymptotic model in section 2.6. The asymptotic model itself, for the chain, is deduced

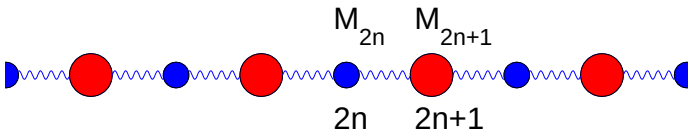

Fig. 1 The diatomic chain of alternating masses considered in section 2.

in section 8 and homogenized models, in the sense that they are set on the macroscale, but with the local structure incorporated through assumption of local symmetries on the elementary cell, are deduced. This all naturally extends to higher dimensional lattice models, and we consider a square lattice explicitly in section 3 deducing the asymptotic structure associated with the Bloch dispersion diagram that allows for considerable physical interpretation. Finally, some closing remarks are drawn together in section 4.

2. Diatomic chain

The simplest lattice model exhibiting band gaps is that of the diatomic lattice which is a classical model, due to Born, for the vibration of atoms in solid state physics as described in (**1**, **2**). For generality, and to illustrate another important point connected to localization, we consider a slightly more general setting with each type of mass varying gradually in spatial location.

2.1 *Formulation*

The masses are connected by a massless string stretched to a constant tension and so the transverse displacement, y_{2n}, y_{2n+1}, of the masses satisfy

$$y_{2n-1} + y_{2n+1} - 2y_{2n} = -M_{2n}\lambda^2 y_{2n} \tag{1}$$

$$y_{2n} + y_{2n+2} - 2y_{2n+1} = -M_{2n+1}\lambda^2 y_{2n+1}. \tag{2}$$

The masses M_{2n}, M_{2n+1} are taken to vary with position so

$$M_{2n} = M_2[1 + \gamma g_{2n}], \qquad M_{2n+1} = M_1[1 + \gamma g_{2n+1}] \tag{3}$$

where M_1, M_2 are constant masses, γ is a constant, g_{2n}, g_{2n+1} are functions that quantify the change in mass with position along the lattice. In the model the tensions, lengths and so on have been scaled out of the problem and the vibration frequency squared is denoted by λ^2. The position of the masses is at $x_{2n} = 2n$ and the displacement is $y_{2n} = y(x_{2n})$. This formulation can easily be generalised to poly-atomic chains and so on, but this adds nothing to the methodology bar to obfuscate the presentation.

2.2 *Bloch waves*

One common setting in which the diatomic chain is encountered is that of an infinite chain, with no defects or spatial variation of the masses ($\gamma = 0$), for which waves travelling through it can be considered over an elementary cell of four masses. The displacements are found using quasi-periodicity conditions relating the phase change at each end of the cell; a Bloch

wavenumber, κ, is introduced as the phase change across a cell. It is convenient to introduce the vector $\mathbf{y}_{2n} = (y_{2n}, y_{2n+1})^T$ where the Floquet-Bloch conditions across the cell are

$$\mathbf{y}_{2n+2} = \exp(i\kappa)\mathbf{y}_{2n}. \tag{4}$$

There is then an explicit dispersion relation,

$$M_1M_2\lambda^4 - 2(M_1+M_2)\lambda^2 + 2(1-\cos\kappa) = 0, \tag{5}$$

relating the frequency to Bloch wavenumber and plots of the dispersion relation are commonplace in the literature and are shown in Figure 2; this is an ideal case against which to verify and explain the asymptotic procedure, although the asymptotics are more versatile than for just generating asymptotic dispersion curves.

Solving the quadratic in λ^2 gives two solutions, the upper branch is the optical branch and the lower one the acoustic branch; these names follow from the wave frequencies of the applications (**1**). There are four eigenvalues, $\lambda_0^2 = 2/(M_1+M_2), 2/M_2, 2/M_1$ and 0, that correspond to standing waves at $\kappa = 0, \pi$. These, and the dispersion curves, are symmetric about the line $(M_1+M_2)/M_1M_2$, c.f. figure 2(a), and thus we need only consider the asymptotics of the upper (optical) branch for the in- and out-of-phase cases. This symmetry arises as the problem is unchanged if we interchange the masses M_1 and M_2 and renumber.

2.3 *Asymptotic solution*

In the diatomic lattice we introduce two scales: a long-scale, on the scale of the grid, characterised by $N \gg 1$ that could be, say, the number of lattice points and $\epsilon = 1/N \ll 1$. We introduce $\eta = 2n/N$ and take η to be a continuous, not discrete, variable. The other scale, the short-scale is taken to be the elementary cell and we specify the integer $m = -1, 0, 1, 2$; the elementary cell corresponds to the masses at $2n$, $2n+1$ and their immediate neighbours. These two-scales are then considered as independent variables and formally we set $y_{2n+m} = y(\eta + m/N, m)$ or more transparently

$$y_{2n+m} = y(\eta + m\epsilon, m) \sim y(\eta, m) + m\epsilon y_\eta(\eta, m) + \frac{(m\epsilon)^2}{2} y_{\eta\eta}(\eta, m) + \dots \tag{6}$$

as $\epsilon \ll 1$. In particular the four displacements used in equations (1),(2) in this notation are $y_{2n-1} = y(\eta - \epsilon, -1)$, $y_{2n} = y(\eta, 0)$, $y_{2n+1} = y(\eta + \epsilon, 1)$ and $y_{2n+2} = y(\eta + 2\epsilon, 2)$. In terms of the two-scale notation, the Bloch conditions (4) are now $y(\eta + 2\epsilon, m) = \exp(ik\epsilon)y(\eta, m)$ where $\kappa = k\epsilon$, that is, the Floquet-Bloch conditions hold on the macroscale.

The asymptotic analysis only uses the displacements at y_{2n} and y_{2n+1}; their neighbouring displacements are related to these two via

$$[y_{2n-1}, y_{2n+2}] = [y(\eta - \epsilon, -1), y(\eta + 2\epsilon, 2)] = (-1)^J [y(\eta - \epsilon, 1), y(\eta + 2\epsilon, 0)] \tag{7}$$

as we assume that the motion, on the microscale of the elementary cell, is that of locally standing waves oscillating in-phase or out-of-phase ($J = 0, 1$ respectively) across the cell (see figure 2 (b) and (c) for an illustration of the displacements for an infinite chain of alternating constant masses).

The mass variation, g_{2n}, g_{2n+1} in (3), is assumed gradual, and identical, in n so $g_{2n} = g_{2n+1} = g(\eta)$, and we also take the constant $\gamma = \epsilon^2\alpha$, that is

$$M_{2n} = M_2[1 + \epsilon^2\alpha g(\eta)], \qquad M_{2n+1} = M_1[1 + \epsilon^2\alpha g(\eta)]. \tag{8}$$

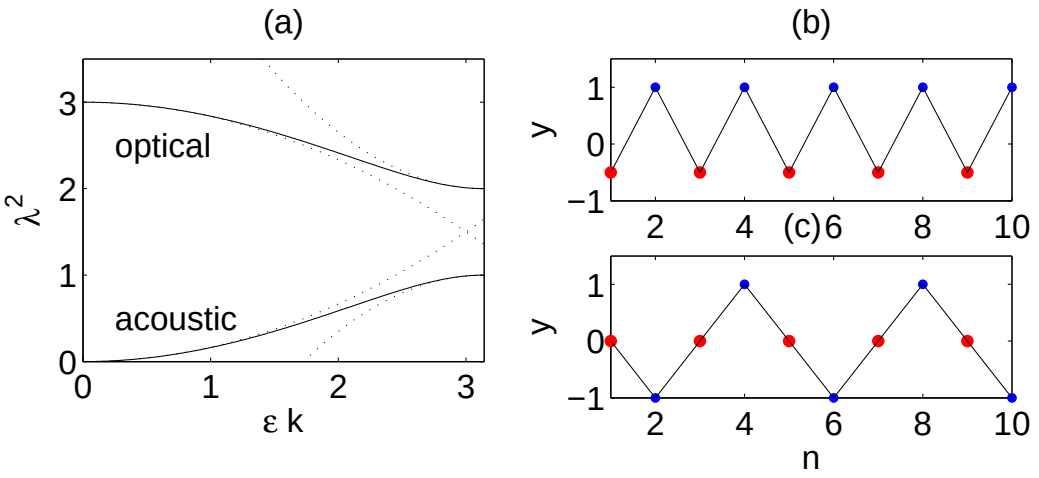

Fig. 2 The Bloch diagram for $M_1 = 2$, $M_2 = 1$. Panel (a) shows the dispersion curves for the diatomic chain ($\gamma = 0$) with the exact curves from (5) solid and asymptotics dotted; the asymptotics are from (2.4) and (2.5) (and their reflections by the symmetry about $\lambda^2 = (M_1 + M_2)/M_1M_2$). Panels (b) and (c) show the displacements of the masses for the optical branch at $k = 0$ and $\epsilon k = \pi$ respectively.

The mass variation is characterised by $g(\eta)$ on the macro-scale this variation is of order ϵ^2; without loss of generality we choose $M_1 \geq M_2$.

In this two-scales notation, equations (1),(2) to order ϵ^2 in matrix form become,

$$[A_0 - \lambda^2 M(1 + \epsilon^2 \alpha g(\eta)) + \epsilon A_1(\partial, \lambda) + \epsilon^2 A_2(\partial^2, \lambda)]\mathbf{y}(\eta) = 0, \tag{9}$$

where ∂ denotes $\partial/\partial\eta$, $\mathbf{y}(\eta) = [y(\eta, 0),\ y(\eta, 1)]^T$ is the displacement vector, M is a diagonal matrix $M = \mathrm{diag}[M_2,\ M_1]$, A_0 is a constant matrix and A_1 and A_2 are matrix differential operators. These matrices depend on periodicity conditions and, therefore, are different for in-phase and out-of-phase cases.

The natural separation of scales leads to a hierarchy of equations in powers of ϵ where the ansatz

$$\mathbf{y}(\eta) = \mathbf{y_0}(\eta) + \epsilon\mathbf{y_1}(\eta) + \epsilon^2\mathbf{y_2}(\eta) + \dots \tag{10}$$

$$\lambda^2 = \lambda_0^2 + \epsilon\lambda_1^2 + \epsilon^2\lambda_2^2 + \dots \tag{11}$$

is adopted. Substituting the ansatz into the lattice equations (8) gives differential-difference equations that are treated order-by-order in ϵ.

2.4 *Optical mode: in-phase*

Standing waves with no phase-shift across the structure lead to periodic conditions for the masses that are $y(\eta, -1) = y(\eta, 1)$ and $y(\eta, 0) = y(\eta, 2)$ (c.f. (7)); at each order the problem on the scale of the cell maintains this relation. The matrices A_0, A_1 and A_2 for the in-phase

problem are

$$A_0 = \begin{pmatrix} 2 & -2 \\ -2 & 2 \end{pmatrix}, \qquad A_1 = \begin{pmatrix} 0 & 0 \\ -2\partial & (2-\lambda_0^2 M_1)\partial \end{pmatrix}, \tag{12}$$

$$A_2 = \begin{pmatrix} 0 & -\partial^2 \\ -2\partial^2 & (1-\frac{1}{2}\lambda_0^2 M_1)\partial^2 - \lambda_1^2 M_1 \partial \end{pmatrix}. \tag{13}$$

We recall that the ansatz (8,8) is introduced and so equations are formed at each order in ϵ and solved in turn.

The separation of scales, and lack of explicit dependence upon η, leads to $\mathbf{y}_0(\eta) = f_0(\eta)\mathbf{Y}_0$. The vector $\mathbf{Y}_0$ is defined on the scale of the elementary cell and displacements of the masses are chosen that lead to standing waves. This also identifies the frequency at which standing waves occur.

Taking the leading term in (8) and substituting $\mathbf{y}_0(\eta) = f_0(\eta)\mathbf{Y}_0$ gives the eigenvalue problem $[A_0 - \lambda_0^2 M]\mathbf{Y}_0 = 0$ from which

$$\mathbf{Y}_0 = (1, -M_2/M_1)^T \quad \text{and} \quad \lambda_0^2 = \frac{2(M_1+M_2)}{M_1 M_2} \tag{14}$$

with $f_0(\eta)$ to be determined. This eigenvector leads to the vibration mode of the masses shown in figure 2(b).

The first order problem allows for an identical separation $\mathbf{y}_1(\eta) = f_1(\eta)\mathbf{Y}_1$ and

$$[A_0 - \lambda_0^2 M]\mathbf{Y}_1 f_1 = \lambda_1^2 M \mathbf{Y}_0 f_0 \tag{15}$$

for which solvability of the matrix system demands $\lambda_1^2 = 0$, with $\mathbf{Y}_1 = (1, -M_2/M_1)^T$ and $f_1(\eta)$ is unknown and not required in the subsequent analysis.

The second order problem, and separation $\mathbf{y}_2(\eta, m) = f_2(\eta)\mathbf{Y}_2$, lead to the matrix system $[A_0 - \lambda_0^2 M]\mathbf{Y}_2 f_2 = R\mathbf{Y_0} f_0$, where R is

$$R = \begin{pmatrix} M_2[\lambda_2^2 + \alpha g(\eta)\lambda_0^2] & \partial^2 \\ 2\partial^2 & M_1[\lambda_2^2 + \alpha g(\eta)\lambda_0^2] + \frac{M_1}{M_2}\partial^2 \end{pmatrix}. \tag{16}$$

Solvability requires $\mathbf{Y}_0^T R \mathbf{Y_0} f_0(\eta) = 0$ and this gives a differential eigenvalue problem

$$\frac{2}{(M_1+M_2)} f_{0\eta\eta} - [\lambda_2^2 + \alpha\lambda_0^2 g(\eta)] f_0 = 0, \tag{17}$$

where $f_{0\eta\eta}$ denotes $\partial^2 f_0/\partial\eta^2$, relating f_0 and λ_2^2. Notably this differential eigenvalue equation is exactly the same, in form, as that found in the long wave high frequency theory leading to trapped modes in bent or deformed acoustic and elastic waveguides (**21**, **22**, **23**, **24**)

For the infinite periodic system, with $\alpha = 0$ so the masses are constant and alternate, we use the Bloch relation (4) to deduce $f_0(\eta) = \exp(ik\eta/2)$ where $\kappa = \epsilon k$ and λ_2^2 is just $\lambda_2^2 = -k^2/[2(M_1+M_2)]$ thus as $k \to 0$, the dispersion relation has the local behaviour that

$$\lambda^2 \sim \frac{2(M_1+M_2)}{M_1 M_2} - \frac{(\epsilon k)^2}{2(M_1+M_2)} + \dots \tag{18}$$

which can also be deduced from the exact relation (5); this asymptotic behaviour is shown in figure 2 (a). The important point behind this example is that given only the standing wave solution to any lattice problem one can perturb off this to deduce the local dispersion behaviour and generate the homogenized equation, (2.4), that encapsulates the local information into a purely macroscopic equation.

2.5 *Optical mode: out-of-phase*

Standing waves with complete phase-shift across the structure lead to periodic conditions for the masses which are $y(\eta,-1) = -y(\eta,1)$ and $y(\eta,0) = -y(\eta,2)$ (c.f. (7)) at each order. Matrices A_0, A_1 and A_2 become

$$A_0 = \begin{pmatrix} 2 & 0 \\ 0 & 2 \end{pmatrix}, \; A_1 = \begin{pmatrix} 0 & -2\partial \\ 2\partial & (2-\lambda^2 M_1)\partial \end{pmatrix}, \; A_2 = \begin{pmatrix} 0 & 0 \\ 2\partial^2 & (1-\tfrac{1}{2}\lambda^2 M_1)\partial^2 \end{pmatrix}. \tag{19}$$

The analysis closely mirrors the in-phase calculation, at leading order

$$\mathbf{Y}_0 = (1,0)^T, \quad \text{and} \quad \lambda_0^2 = \frac{2}{M_2} \tag{20}$$

(with the eigenvector shown in figure 2 (c)) and solutions at first and second order lead to the differential eigenvalue problem that determines $f_0(\eta)$ and λ_2^2 as

$$\frac{2}{(M_1 - M_2)} f_{0\eta\eta} + [\lambda_2^2 + \alpha\lambda_0^2 g(\eta)] f_0 = 0. \tag{21}$$

For $\alpha = 0$ the Bloch relation (4) yields the local behaviour as $\epsilon k \to \pi$ that

$$\lambda^2 \sim \frac{2}{M_2} + \frac{(\epsilon k - \pi)^2}{2(M_1 - M_2)} + \dots \tag{22}$$

which also follows from (5); and is shown in figure 2(a).

The asymptotic behaviour of the acoustic mode follows from symmetry and is not given here.

2.6 *Localization*

If we allow the masses to vary with position, according to (**??**) with $\alpha \neq 0$, then it is possible for discrete defect modes to occur that correspond to modes which are spatially localized (**12**). These localised defect modes can have frequencies that lie in the stop-bands of the structure and the eigenfunctions associated with these frequencies exponentially decay with distance from the defect. The asymptotic technique that is developed here explicitly identifies the frequencies at which these modes occur and their spatial structure. For definiteness we take the mass variation with position as $g(\eta) = \mathrm{sech}^2(\eta)$, that is, the masses alternate between M_1 and M_2 as before but with a gradual variation that is strongest near the origin and decays exponentially as $\eta \to \pm\infty$.

Localized eigensolutions from the difference equations (1,2) are found numerically (they form a generalized eigenvalue problem of the form $A - \lambda^2 M = 0$, for matrices A, M that follow from the difference equations, that is solved using an adaption of the standard QR

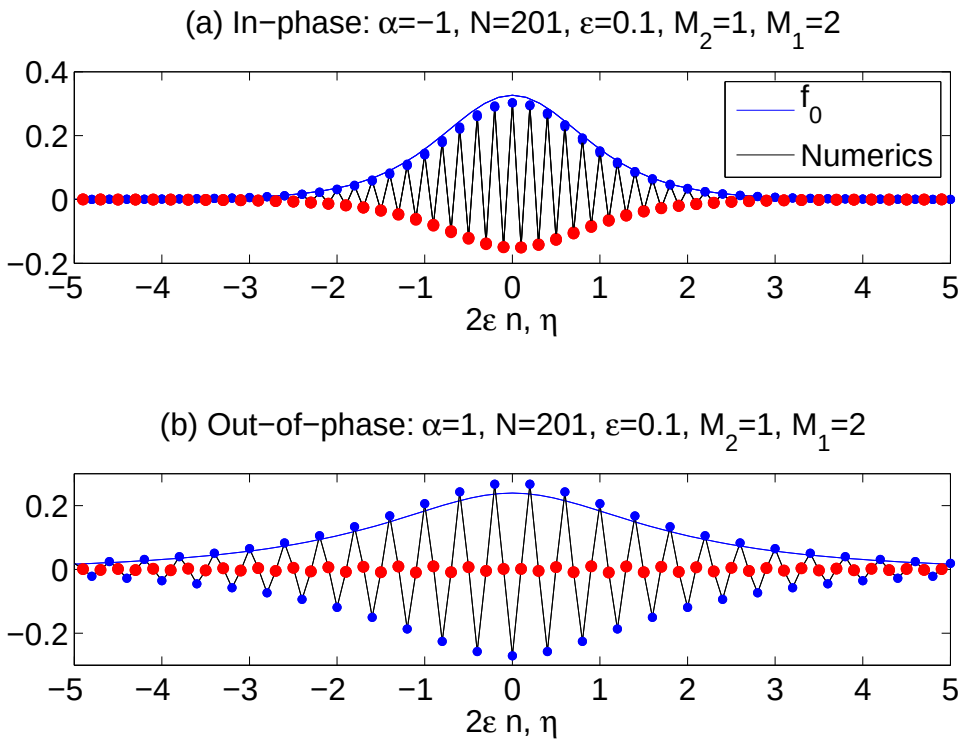

Fig. 3 Localised modes for $M_1 = 2$, $M_2 = 1$ showing the numerical solution of (1,2) versus the f_0 from the asymptotic equations (2.4,2.5) with the $\mathrm{sech}^2(\eta)$ variation. Panel (a) shows a localised in-phase solution for which the numerics give $\lambda^2 \sim 3.01896$ and the asymptotics, (2.6), give $\lambda^2 \sim 3.01880$ that differ in the fourth decimal place. Panel (b) shows the localised out-of-plane eigensolution for $\alpha = 1$ and the numerics give $\lambda^2 = 1.99239$ with the asymptotics, (2.6), as $\lambda^2 = 1.99236$.

matrix eigenvalue algorithm) and typical results are shown in figure 3; the numerics have $\alpha = \pm 1$ and are on a lattice of 201 masses for varying ϵ ($\epsilon = 0.1$ in figure 3). Our interest is in eigensolutions that have frequencies within the stop-bands of the unperturbed structure. These solutions of the exact equations are then compared with those found from our asymptotic differential eigenvalue problems (2.4,2.5) above. As the differential eigenvalue problems are, so far, posed on an infinite domain, the eigenfunctions f_0 arbitrary to within a constant multiple. The lattice we model, is however on a finite range. We can treat this finite domain exactly with the differential eigenvalue problem by noting that $\eta = \epsilon n$. The range for the ODE is $-10 < \eta < 10$ for the example illustrated in figure 3, with $f_0 = 0$ at the end points. This is solved numerically using a Chebyshev spectral collocation scheme to extract both eigenvalue and eigenvector, this provides the f_0, with no ambiguity, to compare with the full eigensolutions from (1,2).

On the infinite interval equations (2.4,2.5), with the specific mass variation we have

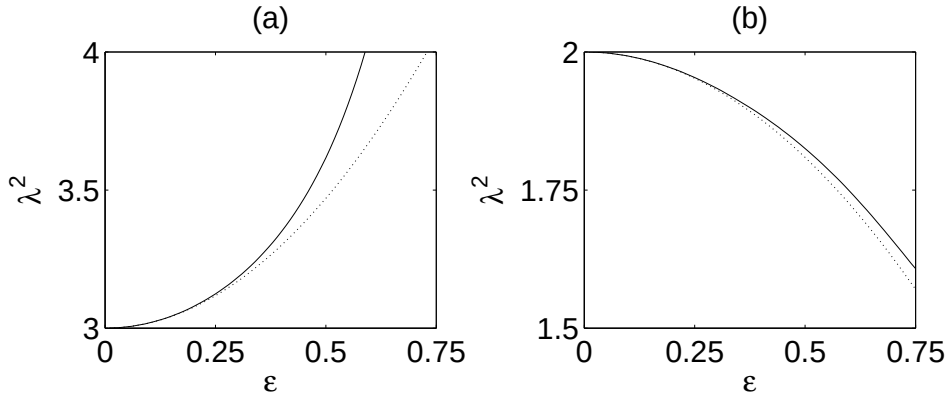

Fig. 4 The localized eigenvalues for $M_1 = 2$, $M_2 = 1$ showing the numerical solution (solid) versus the asymptotics (dotted) from equations (2.6) and (2.6) as ϵ varies. Panels (a) and (b) show the eigenvalues for $\alpha = -1$ and $\alpha = 1$ respectively.

chosen, lead to an exactly solvable differential eigenvalue problem. Equations (2.4,2.5) are of the form

$$\hat{\alpha} f_{\xi\xi} + [\mathrm{sech}^2(\xi) + \hat{\lambda}] f = 0 \tag{23}$$

posed on $-\infty < \xi < \infty$ with f decaying at infinity and $\hat{\alpha}$ constant; this type of eigenvalue problem is exactly that which occurs in the long wave trapping of modes in acoustic or elastic waveguides and the differential eigenvalue problem (2.6) is treated numerically and asymptotically in (**24**). It turns out to actually have an exact solution. Mapping this equation onto $[-1, 1]$ using a tanh substitution turns (2.6) into an associated Legendre equation and the eigenvalues are then extracted explicitly; this is a well-known solvable Schrödinger equation (**25**). The lowest eigenvalue is always negative (for $\hat{\alpha} > 0$) and

$$\hat{\lambda} = -\frac{\hat{\alpha}}{4}\left[1 - \sqrt{\frac{4+\hat{\alpha}}{\hat{\alpha}}}\right]^2. \tag{24}$$

More generally, setting ν to be

$$2\nu = -1 + \sqrt{1 + 4/\hat{\alpha}}$$

gives the negative eigenvalues as

$$\hat{\lambda} = -\hat{\alpha}(\nu - i)^2$$

for $i = 0, 1, \ldots$ although we are primarily interested in the first of these.

For the optical mode, at $k = 0$, with $\lambda_0^2 = 2(M_1 + M_2)/M_1 M_2$ we turn to (2.4) and localised modes require $\alpha < 0$ and the largest eigenfrequency is

$$\lambda^2 = \lambda_0^2 - \epsilon^2 \alpha \lambda_0^2 \frac{\hat{\alpha}}{4}\left[-1 + \sqrt{1 + 4/\hat{\alpha}}\right]^2, \quad \text{where} \quad \hat{\alpha} = -\frac{2}{(M_1 + M_2)\alpha\lambda_0^2}. \tag{25}$$

As $\alpha < 0$, the masses are decreasing as we approach the origin and the correction to λ_0^2 is always positive. One can use the properties of a positive operator and Sturm-Liouville theory, as in (**21**), to make these arguments more rigorous.

At the other end of the optical branch, $\epsilon k = \pi$, and $\lambda_0^2 = 2/M_2$ and we turn to (2.5), for $M_1 \geq M_2$, localised modes require $\alpha > 0$ and the localised eigenfrequency of interest is

$$\lambda^2 = \lambda_0^2 - \epsilon^2 \alpha \lambda_0^2 \frac{\hat{\alpha}}{4}\left[-1 + \sqrt{1 + 4/\hat{\alpha}}\right]^2 \quad \text{and} \quad \hat{\alpha} = \frac{2}{(M_1 - M_2)\alpha\lambda_0^2}. \tag{26}$$

As $\alpha > 0$, the masses are increasing near the origin and the correction to λ_0^2 is negative thereby placing the eigenfrequency in the stop-band of the structure.

The asymptotic eigenfunctions, f_0, are shown in figure 3, for typical values, for both in- and out-of- phase localisation, these are plotted against the numerical eigenfunctions from (1,2). The numerical eigenfunctions clearly oscillate, either in- or out-of- phase for each elementary cell and the asymptotic f_0 provide an envelope for this oscillatory solution; note the full asymptotics give the leading order solution as $\mathbf{y}_{2n} = f_0(\eta)\mathbf{Y_0}$ and $\mathbf{Y}_0$ incorporates the correct oscillatory behaviour. The caption to figure 3 gives the numerical and asymptotic values of the eigenvalues which agree to four decimal places; a more extensive comparison of the eigenvalues versus ϵ is given in figure 4 for both cases.

Variations of the masses in space such that they tend to constant values as $\eta \to \pm\infty$ are not the only types of variation possible. For contrast, we briefly consider $g(\eta) = \eta^2$ so the masses now increase gradually until they tend to infinite values at sufficient distance from the origin. For the in-phase case the localization differential eigenvalue problem is

$$\frac{2}{(M_1 + M_2)} f_{0\eta\eta} - [\lambda_2^2 + \lambda_0^2 \eta^2] f_0 = 0 \tag{27}$$

which can be transformed into Hermite's differential equation, (**22**), from which the eigenvalue correction λ_2^2 is $-2/\sqrt{M_1 M_2}$. Note the correction here is negative and so the eigenvalue does not sit inside the stop-band, but is now outside it. The localised mode still decays exponentially, but it is perhaps less interesting than a mode which lies inside the stop-bands. The asymptotics and numerics again give almost perfect agreement as shown in figure 5 where eigenvalues are given in the caption.

3. Two dimensional theory

The two-scale asymptotic approach naturally works for higher dimensional lattices and we choose to illustrate this using a square two-dimensional lattice structure constructed by alternating masses as shown in figure 6. This structure has considerable symmetry, both geometrically and from interchanging masses, and these symmetries lead to some degeneracies. This square lattice then usefully highlights the wide range of possible behaviours that can arise. For clarity we shall consider only constant, alternating, masses and so localisation phenomena will not occur.

3.1 *Formulation and Bloch waves*

For the square lattice shown in Figure 6 with masses connected by linear strings, and only nearest neighbour interactions, the simplest model, equivalent to anti-plane shear of the

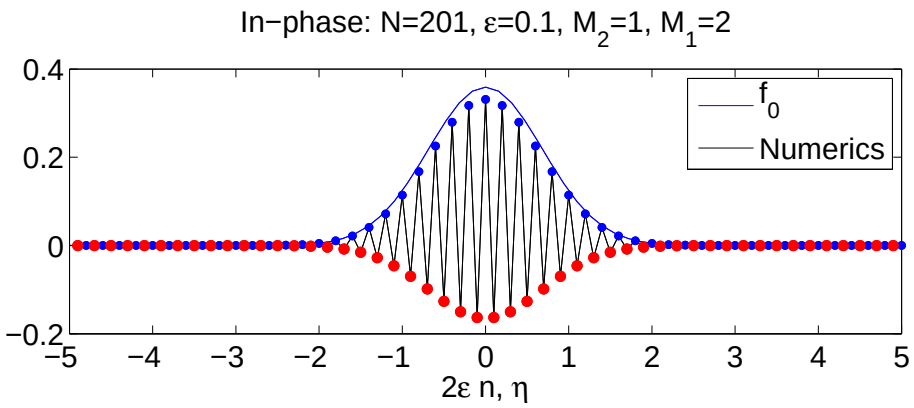

Fig. 5 An in-plane localised solution for the quadratic variation, $g(\eta) = \eta^2$, the eigenvalue is 2.98591 from the numerics and from the asymptotics, (2.6), 2.98585.

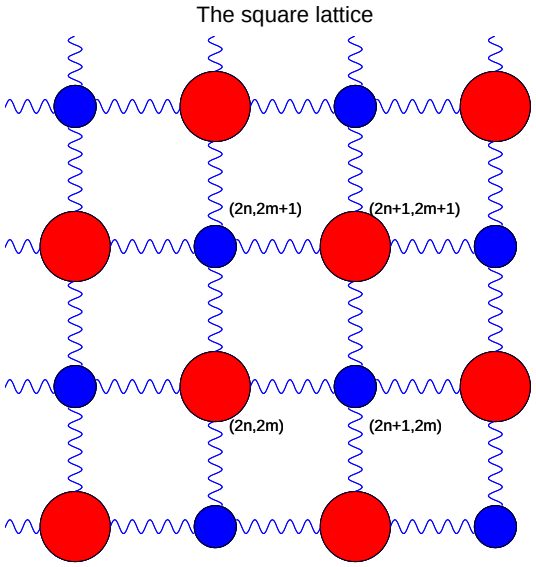

Fig. 6 The square lattice showing an elementary cell of the lattice structure, the masses M_2 (blue) and M_1 (red) alternate.

continuous version, connects the displacements $y_{i,j}$ of the elementary cell of four masses via

$$y_{2n+1,2m} + y_{2n-1,2m} + y_{2n,2m+1} + y_{2n,2m-1} - 4y_{2n,2m} = -M_1\lambda^2 y_{2n,2m} \tag{28}$$

$$y_{2n+2,2m+1} + y_{2n,2m+1} + y_{2n+1,2m+2} + y_{2n+1,2m} - 4y_{2n+1,2m+1} = -M_1\lambda^2 y_{2n+1,2m+1} \tag{29}$$

$$y_{2n+2,2m} + y_{2n,2m} + y_{2n+1,2m+1} + y_{2n+1,2m-1} - 4y_{2n+1,2m} = -M_2\lambda^2 y_{2n+1,2m} \tag{30}$$

$$y_{2n+1,2m+1} + y_{2n-1,2m+1} + y_{2n,2m+2} + y_{2n,2m} - 4y_{2n,2m+1} = -M_2\lambda^2 y_{2n,2m+1} \tag{31}$$

c.f. (**26**) amongst others. Once again there is an inherent symmetry created by interchanging M_1 and M_2 and we can, without loss of generality, choose $M_1 \geq M_2$.

If we consider an infinite medium and utilise the Bloch relation, (4), then

$$\mathbf{y}_{2n+\hat{N},2m+\hat{M}} = \exp(i[\kappa_1\hat{N} + \kappa_2\hat{M}])\mathbf{y}_{2n,2m} \tag{32}$$

holds, for even integers $\hat{N}, \hat{M}$ and a wavenumber vector $\boldsymbol{\kappa} = (\kappa_1, \kappa_2)$. Equation (3.1) leads to the exact dispersion relation given as the eigenvalue problem

$$[A(\boldsymbol{\kappa}) - \lambda^2 M]\mathbf{y}_{2n,2m} = 0. \tag{33}$$

Here $\mathbf{y}_{2n,2m}$ is the displacement vector

$$\mathbf{y}_{2n,2m} = [y_{2n,2m}, y_{2n+1,2m+1}, y_{2n+1,2m}, y_{2n,2m+1}]^T,$$

M is a diagonal matrix, $M = \mathrm{diag}[M_1, M_1, M_2, M_2]$, and $A(\boldsymbol{\kappa})$ is the matrix

$$A(\boldsymbol{\kappa}) = \begin{pmatrix} 4 & 0 & -(1+e^{-2i\kappa_1}) & -(1+e^{-2i\kappa_2}) \\ 0 & 4 & -(1+e^{2i\kappa_2}) & -(1+e^{2i\kappa_1}) \\ -(1+e^{2i\kappa_1}) & -(1+e^{-2i\kappa_2}) & 4 & 0 \\ -(1+e^{2i\kappa_2}) & -(1+e^{-2i\kappa_1}) & 0 & 4 \end{pmatrix} \tag{34}$$

which is Hermitian and thus all eigenvalues are real. This dispersion relation is easily solved numerically and the resulting dispersion curves are shown in Figure 7; it is conventional to show the frequency squared versus wavenumber. In this two-dimensional setting the wavenumber is deduced from the reciprocal lattice, shown as the inset to Figure 7, from which the irreducible Brillouin zone is given by the triangle ABC. At the wavenumbers corresponding to the points A, B and C the lattice vibrates in standing waves and the asymptotic procedure identifies PDEs and thus expansions around these wavenumbers that connect frequency to wavenumber. The square lattice is an interesting structure as it contains several symmetries and these lead to special cases and degeneracies in the analysis, that is, there are repeated eigenvalues (marked as 1 and 5 in Figure 7), flat portions of the dispersion diagram (connecting 3 and 4), as well as distinct eigenvalues (points 2, 3). For the example upon which we have chosen to illustrate the methodology, the square matrix with alternating masses, there is an additional symmetry as the dispersion relation is unaltered by interchanging M_1 with M_2 and this leads to the inherent vertical symmetry about $\lambda^2 = 2/M_1 + 2/M_2$ in Figure 7. Thus we need only consider the upper curves in terms of the asymptotics.

Although we choose to illustrate the asymptotics upon the Bloch wave problem it is notable that the PDEs that we deduce are much more versatile and could, for instance, be used to generate localisation effects or model transient motion on the macro-scale.

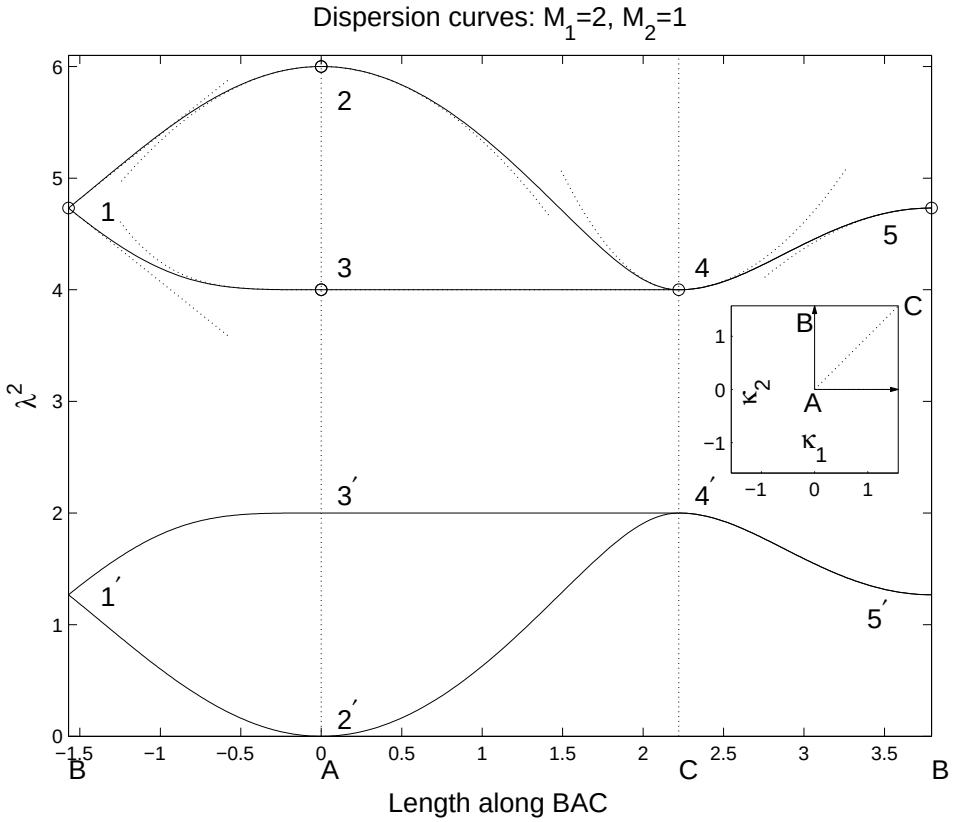

Fig. 7 The dispersion curves for the square lattice: the inset shows shows the reciprocal lattice in $\boldsymbol{\kappa} = (\kappa_1, \kappa_2)$ space, the irreducible Brillouin zone is completely characterised by the triangle ABC. The dispersion curves show the frequency squared versus length along the path $BACB$ for $M_1 = 2$ and $M_2 = 1$. The frequencies at the wavenumbers at B, A, C correspond to various standing waves across the lattice; these are numbered 1 to 5 to allow reference to them in the text. The dotted lines in the upper half of the figure are the asymptotic results.

3.2 *Asymptotics*

We now proceed to treat this problem asymptotically using the natural separation of scales so $y_{2n+m_1,2m+m_2} = y(\eta_1 + m_1\epsilon, \eta_2 + m_2\epsilon, m_1, m_2)$ where the long-scale is characterised by $\epsilon = 1/N \ll 1$ (where N is again a lengthscale associated with the macroscale) with $\eta_1 = 2n/N$ and $\eta_2 = 2m/N$. The short-scale is that of an elementary cell of the structure; in this case the labelled four cell arrangement of figure 7(a). The separation of scales leads to a separation $y(\boldsymbol{\eta} + \mathbf{m}\epsilon, \mathbf{m})$ where $\boldsymbol{\eta} = (\eta_1, \eta_2)$ and $\mathbf{m} = (m_1, m_2)$. For the four points that make the elementary cell

$$\mathbf{y}_{2n,2m} = [y(\eta_1, \eta_2, 0, 0), y(\eta_1 + \epsilon, \eta_2 + \epsilon, 1, 1), y(\eta_1 + \epsilon, \eta_2, 1, 0), y(\eta_1, \eta_2 + \epsilon, 0, 1)]^T. \quad (35)$$

There are four fundamental cases to consider: (i) standing waves set up with periodic

boundary conditions both in n and m (horizontally and vertically) for the elementary cell, that is, waves are perfectly in-phase on the scale of the cell. (ii) and (iii) Standing waves are in-phase in one direction, but out-of-phase in another, and finally (iv) standing waves out-of-phase across the cell. Cases (ii) and (iii), from the symmetry of the structure are identical to within a rotation.

The standing wave assumptions of periodicity and anti-periodicity (completely out-of-phase) across the cell impose constraints upon the displacements of the masses lying outside the elementary cell, but which appear in (3.1)-(3.1). A concise notation is that

$$[y_{2n-1,2m}, y_{2n-1,2m+1}, y_{2n+2,2m}, y_{2n+2,2m+1}] = (-1)^{J_1}$$

$$[y(\eta_1-\epsilon,\eta_2,1,0), y(\eta_1-\epsilon,\eta_2+\epsilon,1,1), y(\eta_1+2\epsilon,\eta_2,0,0), y(\eta_1+2\epsilon,\eta_2+\epsilon,0,1)] \quad (36)$$

and

$$[y_{2n,2m-1}, y_{2n+1,2m-1}, y_{2n,2m+2}, y_{2n+1,2m+2}] = (-1)^{J_2}$$

$$[y(\eta_1,\eta_2-\epsilon,0,1), y(\eta_1+\epsilon,\eta_2-\epsilon,1,1), y(\eta_1,\eta_2+2\epsilon,0,0), y(\eta_1+\epsilon,\eta_2+2\epsilon,1,0)] \quad (37)$$

where $J_i = 0$ if the standing wave is periodic in the direction η_i for $i = 1, 2$, and $J_i = 1$ for standing waves completely out-of-phase in direction η_i. Thus in the cases (i)-(iv) above: $J_1 = J_2 = 0$; $J_1 = 1$ $J_2 = 0$; $J_1 = 0$ $J_2 = 1$; $J_1 = J_2 = 1$ respectively.

We seek a solution in the limit as $\epsilon \to 0$ and Taylor expand with

$$y(\eta_1+\alpha_1\epsilon,\eta_2+\alpha_2\epsilon,\mathbf{m}) = y(\boldsymbol{\eta},\mathbf{m}) + \epsilon[\alpha_1 y_{\eta_1}(\boldsymbol{\eta},\mathbf{m}) + \alpha_2 y_{\eta_2}(\boldsymbol{\eta},\mathbf{m}) +$$

$$\frac{\epsilon^2}{2}[\alpha_1^2 y_{\eta_1\eta_1}(\boldsymbol{\eta},\mathbf{m}) + 2\alpha_1\alpha_2 y_{\eta_1\eta_1}(\boldsymbol{\eta},\mathbf{m}) + \alpha_2^2 y_{\eta_2\eta_2}(\boldsymbol{\eta},\mathbf{m})] + \dots \quad (38)$$

To order ϵ^2, the differential-matrix problem

$$[A_0 - \lambda^2 M + \epsilon A_1(\partial_i,\lambda) + \epsilon^2 A_2(\partial_i\partial_j,\lambda)]\mathbf{y}(\boldsymbol{\eta}) = 0 \quad (39)$$

emerges where $\mathbf{y}(\boldsymbol{\eta})$ is the displacement vector

$$\mathbf{y}(\boldsymbol{\eta}) = [y(\boldsymbol{\eta},0,0), y(\boldsymbol{\eta},1,1), y(\boldsymbol{\eta},1,0), y(\boldsymbol{\eta},0,1)]^T.$$

For brevity we use ∂_i as a shorthand notation for $\partial/\partial\eta_i$ (for $i = 1, 2$). In $\mathbf{y}(\boldsymbol{\eta})$ we drop the explicit dependence on the second scale $\mathbf{m}$ as we can ultimately limit ourselves to dealing with the elementary cell of the four fundamental masses used in $\mathbf{y}$. In (3.2), M is a diagonal matrix $M = \mathrm{diag}[M_1, M_1, M_2, M_2]$, A_0 is a constant matrix, and A_1, A_2 are matrix differential operators that are different for each of the J_i above. The asymptotic expansions

$$\mathbf{y}(\boldsymbol{\eta}) = \mathbf{y}_0(\boldsymbol{\eta}) + \epsilon\mathbf{y}_1(\boldsymbol{\eta}) + \epsilon^2\mathbf{y}_2(\boldsymbol{\eta}) + \dots \quad (40)$$

$$\lambda^2 = \lambda_0^2 + \epsilon\lambda_1^2 + \epsilon^2\lambda_2^2 + \dots \quad (41)$$

are adopted.

3.3 *Case (i): in-phase in both directions*

The matrix A_0 is

$$A_0 = \begin{pmatrix} 4 & 0 & -2 & -2 \\ 0 & 4 & -2 & -2 \\ -2 & -2 & 4 & 0 \\ -2 & -2 & 0 & 4 \end{pmatrix} \tag{42}$$

from which the leading order problem that defines the standing wave solutions is $(A_0 - \lambda_0^2 M)\mathbf{y}_0(\boldsymbol{\eta}) = 0$. which has eigenvalues $\lambda_0^2 = 0$, $4(M_2 + M_1)/(M_1M_2)$, $4/M_1$, $4/M_2$ and associated eigenvectors $\mathbf{y}_0(\boldsymbol{\eta}) = f_0(\boldsymbol{\eta})\mathbf{Y}_0$ with

$$\mathbf{Y}_0 = (1,1,1,1)^T, (1,1,-M_1/M_2,-M_1/M_2)^T, (1,-1,0,0)^T \text{ and } (0,0,-1,1)^T \tag{43}$$

respectively. As noted earlier there is a symmetry of the problem, interchanging M_2 and M_1, and we need only consider the behaviour near the largest two eigenvalues: $4(M_2 + M_1)/(M_1M_2)$ and $4/M_2$. The matrices A_1 and A_2, for use in (3.2), are

$$A_1 = -\begin{pmatrix} 0 & 0 & 0 & 0 \\ 0 & \mathcal{M}_1(\partial_1+\partial_2) & 2(\partial_1+\partial_2) & 2(\partial_1+\partial_2) \\ 2\partial_1 & 2\partial_1 & \mathcal{M}_2\partial_1 & 0 \\ 2\partial_2 & 2\partial_2 & 0 & \mathcal{M}_2\partial_2 \end{pmatrix} \tag{44}$$

$$A_2 = -\begin{pmatrix} 0 & 0 & \partial_1^2 & \partial_2^2 \\ 0 & \mathcal{M}_1\left(\frac{\partial_1^2}{2} + \partial_1\partial_2 + \frac{\partial_2^2}{2}\right) + M_1\lambda_1^2(\partial_1+\partial_2) & \partial_1^2 + 2(\partial_1\partial_2+\partial_2^2) & 2(\partial_1^2+\partial_1\partial_2)+\partial_2^2 \\ 2\partial_1^2 & \partial_1^2+\partial_2^2 & \mathcal{M}_2\partial_1^2/2 + M_2\lambda_1^2\partial_1 & 0 \\ 2\partial_2^2 & \partial_1^2+\partial_2^2 & 0 & \mathcal{M}_2\partial_2^2/2 + M_2\lambda_1^2\partial_2 \end{pmatrix} \tag{45}$$

where the combinations $\mathcal{M}_i = M_i\lambda_0^2 - 4$, for $i = 1, 2$, are the only places where the leading order eigenvalue appears.

We now consider the asymptotic behaviour near the eigenvalues $\lambda_0^2 = 4(M_2 + M_1)/(M_1M_2)$ and $\lambda_0^2 = 4/M_2$ in detail; a schematic of the standing wave oscillations of the masses for these cases is given in Figure 8.

At leading order $\lambda_0^2 = 4(M_2 + M_1)/(M_1M_2)$, and $\mathbf{Y}_0 = (1, 1, -M_1/M_2, -M_1/M_2)^T$. To first order the equation that determines $\mathbf{y}_1$ and the correction to the frequency, λ_1^2, is

$$(A_0 - \lambda_0^2 M)\mathbf{y}_1(\boldsymbol{\eta}) = -(A_1 - \lambda_1^2 M)f_0(\boldsymbol{\eta})\mathbf{Y}_0.$$

The matrix problem is only solvable if $\mathbf{Y}_0^T(A_1 - \lambda_1^2 M)\mathbf{Y}_0 f_0 = 0$ which forces $\lambda_1^2 = 0$ and $\mathbf{y}_1(\boldsymbol{\eta}) = f_1(\boldsymbol{\eta})\mathbf{Y}_0$. The second order problem is that

$$(A_0 - \lambda_0^2 M)\mathbf{y}_2(\boldsymbol{\eta}) = -[A_1 f_1(\boldsymbol{\eta}) + (A_2 - \lambda_2^2 M)f_0(\boldsymbol{\eta})]\mathbf{Y}_0 \tag{46}$$

and the solvability condition leads to a partial differential eigenvalue problem connecting f_0 and λ_2^2,

$$\nabla^2 f_0 - \frac{(M_1 + M_2)}{2}\lambda_2^2 f_0 = 0, \tag{47}$$

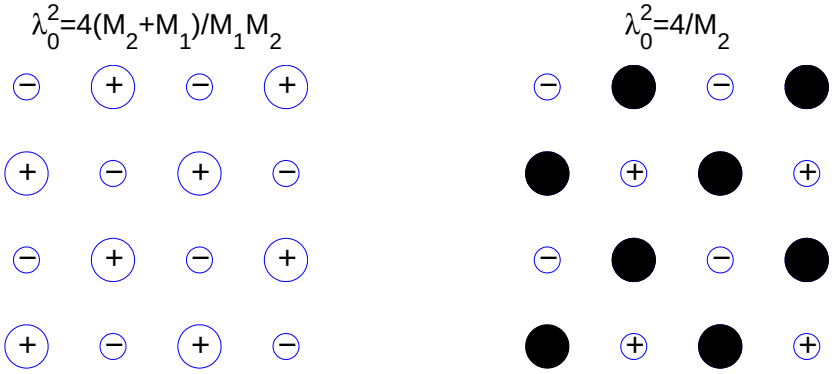

Fig. 8 The standing wave pattern for the two in-phase standing wave cases considered in section 3.3: stationary masses are indicated by black circles, the relative amplitude of the positive and negative displacements follow from the eigenvector values. The larger (smaller) circles correspond to masses M_1 and M_2 respectively.

where $\nabla^2 = \partial_1^2 + \partial_2^2$. This PDE now completely captures the asymptotic behaviour of this lattice structure for frequencies close to $\lambda_0^2 = 4(M_1 + M_2)/M_1M_2$.

For infinite periodic systems satisfying the quasi-periodicity (Bloch) conditions, (3.1),

$$f_0(\boldsymbol{\eta}) = \exp[i(k_1\eta_1 + k_2\eta_2)] \tag{48}$$

where $\boldsymbol{\kappa} = \epsilon\mathbf{k}$. For the dispersion diagram in Figure 7(c) this corresponds to the behaviour near the point labelled 2. From (3.3) the asymptotics are

$$\lambda^2 \sim \frac{4(M_1 + M_2)}{M_1M_2} - \frac{2(k_1^2 + k_2^2)}{(M_1 + M_2)} + \dots \tag{49}$$

so the behaviour is locally quadratic in the wavenumber and holds as the point 2 is approached from either direction; these asymptotics are shown in Figure 7(c). From symmetry, the asymptotic behaviour near the point labelled $2'$ is controlled by $\nabla^2 f_0 + (M_1 + M_2)\lambda_2^2 f_0/2 = 0$ with $\lambda_0^2 = 0$. This point is where one would conventionally think of long waves, namely where $\boldsymbol{\kappa} \sim 0$, and where classical low-frequency homogenization would be applicable. The asymptotics near the point $2'$ are readily deduced; this can be done near all the primed points and we do not mention this again.

For $\lambda_0^2 = 4/M_2$ the eigenvector $\mathbf{Y}_0 = (0, 0, -1, 1)^T$ and the matrices A_1 and A_2 simplify to have several zero elements. The leading order solution is that $\mathbf{y}_0 = \mathbf{Y}_0 f_0(\boldsymbol{\eta})$, and at first order solvability gives $\lambda_1 = 0$ and $(A_0 - \lambda_0^2 M)\mathbf{y}_1(\boldsymbol{\eta}) = 0$ from which $\mathbf{y}_1(\eta) = \mathbf{Y}_0 f_1(\boldsymbol{\eta})$ again. Proceeding to second order gives

$$[A_0 - \lambda_0^2 M]\mathbf{y}_2 = -[A_1 f_1 + (A_2 - \lambda_2^2 M) f_0]\mathbf{Y}_0$$

and from the simplified form of A_2 the solvability condition gives $\lambda_2^2 = 0$. Thus, for this case we anticipate the partial differential equation that we shall deduce is of higher order than second, and that the local behaviour for the Bloch problem near this eigenvalue will no

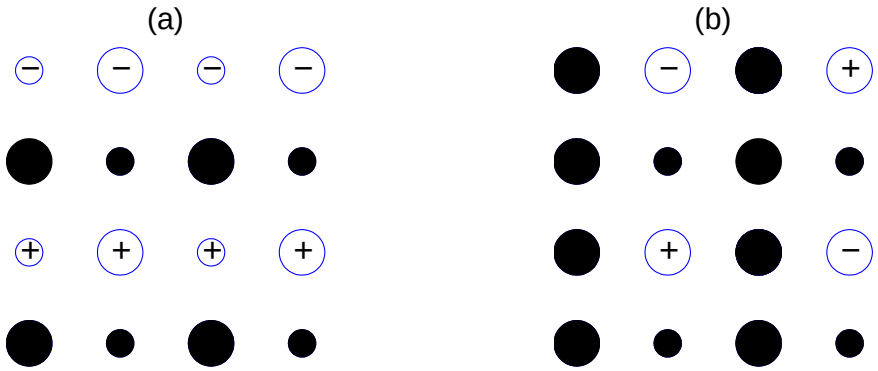

Fig. 9 The standing wave pattern for, panel (a), the standing wave cases considered in section 3.4 and in panel (b) for that is section 3.5: stationary masses are indicated by black circles, the relative amplitude of the positive and negative displacements follow from the eigenvector values. The larger (smaller) circles correspond to masses M_1 and M_2 respectively.

longer be simply quadratic. The second order problem is then solved to give $\mathbf{y}_2$ explicitly as

$$\mathbf{y}_2 = f_2(\boldsymbol{\eta})\mathbf{Y}_0 + \frac{M_2(\partial_1^2 - \partial_2^2)}{4(M_2 - M_1)} f_0(\boldsymbol{\eta})\mathbf{Y}_2, \quad \text{with} \quad \mathbf{Y}_2 = (-1, 1, 0, 0)^T. \tag{50}$$

Proceeding to yet higher order one discovers that the matrix differential operators A_3 and A_4 play no role, and at third order $\lambda_3^2 = 0$, with the fourth order problem yielding a solvability condition

$$\mathbf{Y}_0^T[\lambda_4^2 M\mathbf{y}_0 - A_2\mathbf{y}_2] = 0. \tag{51}$$

The fourth order partial differential eigenvalue problem connecting f_0 and the correction to the eigenvalue as λ_4^2 follows as

$$\frac{1}{4(M_2 - M_1)}\left[\nabla^4 f_0 - 4\partial_1^2\partial_2^2 f_0\right] + \lambda_4^2 f_0 = 0. \tag{52}$$

We now consider the infinite Bloch problem and use the Bloch conditions (3.3) from which we get

$$\lambda^2 \sim \frac{4}{M_2} - \frac{1}{4(M_2 - M_1)}[(\kappa_1^2 + \kappa_2^2)^2 - 4\kappa_1^2\kappa_2^2] + \dots \tag{53}$$

so the frequency dependence upon wavenumber is locally quartic and these asymptotics are shown in Figure 7, but appear different depending upon the direction in which one approaches the point 3. Notably along AC in the Brillouin zone, $k_1 = k_2$ and the correction term vanishes so $\lambda^2 \sim \lambda_0^2$ and the dispersion curve is locally flat exactly as in figure 7; this flat curve suggests that the group velocity is zero for this range of wavenumbers and has relevance to physical applications such as slow light (**27**).

3.4 *Case (ii): periodic in η_1 and anti-periodic in η_2*

Case (iii) which is based around standing waves periodic in η_2 and anti-periodic in η_1 is a simple rotation of the present case, so is absorbed into this section and not treated separately. The solution methodology follows that of case (i), however there is an interesting, and quite different, degenerative situation whereby double eigenvalues appear and so we treat it in detail.

The matrix A_0 is now

$$A_0 = \begin{pmatrix} 4 & 0 & -2 & 0 \\ 0 & 4 & 0 & -2 \\ -2 & 0 & 4 & 0 \\ 0 & -2 & 0 & 4 \end{pmatrix} \tag{54}$$

from which the leading order problem that defines the standing wave solutions is $(A_0 - \lambda_0^2 M)\mathbf{y}_0(\boldsymbol{\eta}) = 0$ which has two double eigenvalues

$$\lambda_0^2 = \frac{2}{M_1 M_2}\left(M_1 + M_2 \pm \sqrt{M_1^2 + M_2^2 - M_1 M_2}\right) \tag{55}$$

and associated eigenvectors

$$\mathbf{Y}_0^{(1)} = (1, 0, \beta, 0)^T \quad \text{and} \quad \mathbf{Y}_0^{(2)} = (0, 1, 0, \beta)^T. \tag{56}$$

The constant β is $\beta = 2/[4 - M_2\lambda_0^2]$, and we use superscripts on the eigenvectors as we shall require both of them. A schematic of one of the standing wave oscillations of the masses is given in Figure 9 (a); the other being just a vertical translation of the one shown. We concentrate only on the behaviour near the largest eigenvalue which comes from the positive branch of (3.4). As the eigenvalues are multiple the leading order solution involves both eigenvectors

$$\mathbf{y}_0 = f_0^{(1)}(\boldsymbol{\eta})\mathbf{Y}_0^{(1)} + f_0^{(2)}(\boldsymbol{\eta})\mathbf{Y}_0^{(2)} \tag{57}$$

where there are now two unknown functions $f_0^{(i)}(\boldsymbol{\eta})$ for $i = 1, 2$.

The first order problem yields

$$[A_0 - \lambda_0^2 M]\mathbf{y}_1 = -[A_1 - \lambda_1^2 M][f_0^{(1)}(\boldsymbol{\eta})\mathbf{Y}_0^{(1)} + f_0^{(2)}(\boldsymbol{\eta})\mathbf{Y}_0^{(2)}] \tag{58}$$

where the matrix differential operator A_1 is

$$A_1 = -\begin{pmatrix} 0 & 0 & 0 & 2\partial_2 \\ 0 & \mathcal{M}_1(\partial_1 + \partial_2) & -2\partial_2 & 2(\partial_1 + \partial_2) \\ 2\partial_1 & 2\partial_2 & \mathcal{M}_2\partial_1 & 0 \\ -2\partial_2 & 2\partial_2 & 0 & \mathcal{M}_2\partial_2 \end{pmatrix}. \tag{59}$$

There are then two solvability equations

$$\mathbf{Y}_0^{(i)T}[A_1 - \lambda_1^2 M][f_0^{(1)}(\boldsymbol{\eta})\mathbf{Y}_0^{(1)} + f_0^{(2)}(\boldsymbol{\eta})\mathbf{Y}_0^{(2)}] = 0 \tag{60}$$

for $i = 1, 2$ that do not give $\lambda_1^2 = 0$, as in case (i). We therefore expect the correction to

the eigenvalue to be linear in k for the Bloch problem. The result is that we have a coupled system of partial differential eigenvalue problems for $f_0^{(1)}(\boldsymbol{\eta})$, $f_0^{(2)}(\boldsymbol{\eta})$ and λ_1^2:

$$\lambda_1^2[M_1+\beta^2 M_2]f_0^{(1)}+4\beta\frac{\partial f_0^{(2)}}{\partial\eta_2}=0 \tag{61}$$

$$\lambda_1^2[M_1+\beta^2 M_2]f_0^{(2)}-4\beta\frac{\partial f_0^{(1)}}{\partial\eta_2}=0. \tag{62}$$

We now turn to the Bloch, infinite lattice, problem and note that the in-phase, in η_1, and out-of-phase, in η_2, conditions force

$$f_0^{(j)}(\boldsymbol{\eta})=\hat{f}_0^{(j)}\exp\left[i\left(k_1\eta_1+\left(k_2+\frac{\pi}{2\epsilon}\right)\eta_2\right)\right], \tag{63}$$

for some constants $\hat{f}_0^{(j)}$, $j=1,2$. Substitution in equations (3.4,3.4) lead to the asymptotic dispersion relation

$$\lambda^2=\lambda_0^2\pm\frac{4\beta\left(\kappa_2+\pi/2\right)}{M_1+\beta^2M_2}+\dots \tag{64}$$

that is, these are straight lines independent of k_1; these asymptotics are shown in figure 7 at the point 1. From the construction of the Brillouin zone, in figure 7, κ_2 actually runs from $-\pi/2$ to 0 on BA. From the periodicity of the irreducible Brillouin zone these asymptotics should also represent the dispersion curve at the other end of the Brillouin zone, near point 5. However, they apparently do not. The reason is that the path taken, BC, on the rightmost segment of the Brillouin zone has

$$f_0^{(j)}(\boldsymbol{\eta})=\hat{f}_0^{(j)}\exp\left[i\left(k_1\eta_1+\left(k_2-\frac{\pi}{2\epsilon}\right)\eta_2\right)\right], \tag{65}$$

and $\kappa_2=\pi/2$ with $0\le\kappa_1<\pi/2$ and so is independent of η_2. Thus the first order correction is identically zero and one must proceed to the next term in the expansion, and for this we require A_2

$$A_2=-\begin{pmatrix} 0 & 0 & \partial_1^2 & 0\\ 0 & \mathcal{M}_1\left(\frac{\partial_1^2}{2}+\partial_1\partial_2+\frac{\partial_2^2}{2}\right) & -2(\partial_1\partial_2+\partial_2^2) & 2(\partial_1^2+\partial_1\partial_2)+\partial_2^2\\ 2\partial_1^2 & 2\partial_1\partial_2 & \mathcal{M}_2\partial_1^2/2 & 0\\ -2\partial_2^2 & \partial_1^2+\partial_2^2 & 0 & \mathcal{M}_2\partial_2^2/2 \end{pmatrix}. \tag{66}$$

The solvability condition

$$\mathbf{Y}_0^{(i)T}[A_2-\lambda_2^2M][f_0^{(1)}(\boldsymbol{\eta})\mathbf{Y}_0^{(1)}+f_0^{(2)}(\boldsymbol{\eta})\mathbf{Y}_0^{(2)}]=0, \tag{67}$$

for $i=1,2$, occurs from which, for this degenerate case, when the structure is locally invariant in η_2, we have the decoupled equations

$$\frac{2\beta}{(M_1+\beta^2M_2)}\frac{\partial^2 f_0^{(j)}}{\partial\eta_1^2}+\lambda_2^2f_0^{(j)}=0 \tag{68}$$

for $j=1,2$.

Returning to the Bloch problem, equations (3.4) have identical coefficients and thus we expect a single, repeated, dispersion curve rather than a pair. The local dispersion equation, from (3.4) is thus

$$\lambda^2 = \lambda_0^2 + \frac{2\beta\kappa_1^2}{M_1 + \beta^2 M_2} + \dots \tag{69}$$

and this is shown in figure 7 as the asymptotic result near the point 5 and explains the single curve observed along BC (in the upper half of the figure).

3.5 *Case (iv): anti-periodic in both η_1 and η_2*

In this case the matrix A_0 is simply $A_0 = 4I$ where I is the identity matrix. The leading order problem again has two double eigenvalues

$$\lambda_0^2 = 4/M_1, \quad \text{and} \quad 4/M_2$$

and eigenvectors with

$$\mathbf{Y}_0 = (1,0,0,0)^T, (0,1,0,0)^T, (0,0,1,0)^T, (0,0,0,1)^T. \tag{70}$$

A schematic of one of the standing wave oscillations of the masses for these cases is given in Figure 9 (b); the others being just vertical or horizontal translations of the one shown. In this case most of the masses remain stationary with the pattern repeating on twice the original elementary cell. From the symmetry inherent in the problem we need only consider the neighbourhood of the larger eigenvalue, $\lambda_0^2 = 4/M_2$, in detail.

As λ_0^2 is a double eigenvalue the leading order solution is

$$\mathbf{y}_0 = f_0^{(1)}(\boldsymbol{\eta})\mathbf{Y}_0^{(1)} + f_0^{(2)}(\boldsymbol{\eta})\mathbf{Y}_0^{(2)} \tag{71}$$

with $\mathbf{Y}_0^{(1)} = (0,0,1,0)^T$ and $\mathbf{Y}_0^{(2)} = (0,0,0,1)^T$. Moving to the next order the solvability condition is

$$\mathbf{Y}_0^{(i)T}[A_1 - \lambda_1^2 M]\mathbf{y}_0 = 0 \tag{72}$$

where A_1 is

$$A_1 = -\begin{pmatrix} 0 & 0 & 2\partial_1 & 2\partial_2 \\ 0 & \mathcal{M}_1(\partial_1+\partial_2) & -2\partial_2 & -2\partial_1 \\ -2\partial_1 & 2\partial_2 & \mathcal{M}_2\partial_1 & 0 \\ -2\partial_2 & 2\partial_1 & 0 & \mathcal{M}_2\partial_2 \end{pmatrix}. \tag{73}$$

Performing the algebra in (3.5) gives $\lambda_1^2 = 0$ and $\mathbf{y}_1$ is determined from

$$[A_0 - \lambda_0^2 M]\mathbf{y}_1 = -A_1\mathbf{y}_0 \tag{74}$$

as

$$\mathbf{y}_1 = f_1^{(1)}(\boldsymbol{\eta})\mathbf{Y}_0^{(1)} + f_1^{(2)}(\boldsymbol{\eta})\mathbf{Y}_0^{(2)} + \mathbf{Y}_1^{(1)} f_0^{(1)}(\boldsymbol{\eta}) + \mathbf{Y}_1^{(2)} f_0^{(2)}(\boldsymbol{\eta}). \tag{75}$$

The first two terms are the homogeneous solution and play no further role, the last two terms have

$$\mathbf{Y}_1^{(1)} = \frac{M_2}{2(M_2 - M_1)}[\partial_1, -\partial_2, 0, 0]^T,$$

$$\mathbf{Y}_1^{(2)} = \frac{M_2}{2(M_2 - M_1)}[\partial_2, -\partial_1, 0, 0]^T.$$

As $\lambda_1^2 = 0$ the first correction to the eigenvalue is zero, despite there being a double eigenvalue, and so we move to second order. The A_2 matrix plays a minor role,

$$A_2 = -\begin{pmatrix} 0 & 0 & 0 & 0 \\ 0 & \mathcal{M}_1\left(\frac{\partial_1^2}{2} + \partial_1\partial_2 + \frac{\partial_2^2}{2}\right) & -2(\partial_1\partial_2 + \partial_2^2) & -2(\partial_1^2 + \partial_1\partial_2) \\ -2\partial_1^2 & 2\partial_1\partial_2 & 0 & 0 \\ -2\partial_2^2 & 2\partial_1\partial_2 & 0 & 0 \end{pmatrix}, \tag{76}$$

as the elements that would lead to it entering the calculation are all zero.

The solvability condition gives

$$\mathbf{Y}_0^{(i)T} A_1[\mathbf{Y}_1^{(1)} f_0^{(1)} + \mathbf{Y}_1^{(2)} f_0^{(2)}] - \lambda_2^2 M_2 f_0^{(i)} = 0 \tag{77}$$

for $i = 1, 2$ and thus the coupled partial differential eigenvalue problems

$$\frac{1}{(M_1 - M_2)}[\nabla^2 f_0^{(i)} + 2\partial_1\partial_2 f_0^{(j)}] + \lambda_2^2 f_0^{(i)} = 0 \tag{78}$$

for $i, j = 1, 2$ and $i \neq j$ are found connecting the $f_0^{(i)}$ with the eigenvalue correction λ_2^2.

The infinite Bloch lattice in the vicinity of C now has the quasi-periodicity conditions

$$f_0^{(j)}(\boldsymbol{\eta}) = \hat{f}_0^{(j)} \exp\left[i\left(\left(k_1 - \frac{\pi}{2\epsilon}\right)\eta_1 + \left(k_2 - \frac{\pi}{2\epsilon}\right)\eta_2\right)\right], \tag{79}$$

for $j = 1, 2$ and $\hat{f}_0^{(j)}$ constant. We now aim to extract the asymptotic behaviour near point 4 in figure 7. From the coupled equations (3.5) we get

$$\lambda_2^2 = -\frac{1}{(M_2 - M_1)}\left[\left(k_1 - \frac{\pi}{2\epsilon}\right) \pm \left(k_2 - \frac{\pi}{2\epsilon}\right)\right]^2. \tag{80}$$

Along CB $\kappa_2 = \epsilon k_2 = \pi/2$ and the single branch

$$\lambda^2 = \lambda_0^2 - \frac{(\kappa_1 - \pi/2)^2}{(M_2 - M_1)} \tag{81}$$

is found. Along CA, $\kappa_1 = \kappa_2$, and one solution is that $\lambda_2^2 = 0$ and $\lambda \sim \lambda_0^2$ to this order and the corresponding curve in figure 7 is flat; this is the straight line joining points 4 and 3. Alternatively

$$\lambda = \lambda_0^2 - \frac{(2\kappa_1 - \pi)^2}{(M_2 - M_1)} \tag{82}$$

which is the asymptotic behaviour for the curve connecting the point 4 with the point 2.

3.6 *Homogenized Models*

The two-scale approach we have developed leads to a variety of homogenized lattice models, see equations (3.3), (3.3), (3.4,3.4), (3.4), and (3.5). Apart from the second-order equation

(3.3) containing a Laplace operator, all of them take a rather sophisticated form due to various degenerations related to the symmetries of the original discrete lattice formulation (3.1)-(3.1).

It is worth mentioning that the derived models are valid in more general settings, than the infinite Bloch case that we chose to illustrate the method upon, including external transient loading. As an example, consider equation (3.3). In this case the effect of discrete macro-scale loading may be incorporated as an inhomogeneous term $\epsilon^4\mathbf{P}(\boldsymbol{\eta})$, where $\mathbf{P} = [P_1, P_2, P_3, P_4]^T$, in the right-hand side of the matrix equation (3.2). Let us also take into account transient motions satisfying the asymptotic relation

$$\frac{\partial^2 f_0}{\partial t^2} - \frac{4}{M_2} f_0 \sim \epsilon^4 f_0 \tag{83}$$

where t is time; for transient loadings, with a broad frequency spectrum, the developed theory describes only a part of the overall response with the variation in time given by the last formula. The transient problem, and the subsequent treatment of the asymptotic ordinary differential equations, is very close to that for thin plates detailed in (**28**, **29**).

By introducing dimensional co-ordinates $x_i = l\eta_i$, with l denoting the distance between masses, we finally get

$$\frac{l^4}{4(M_2 - M_1)} \left(\frac{\partial^4 f_0}{\partial x_1^4} + \frac{\partial^4 f_0}{\partial x_2^4} - 2\frac{\partial^4 f_0}{\partial x_1^2 \partial x_2^2} \right) + \frac{\partial^2 f_0}{\partial t^2} - \frac{4}{M_2} f_0 = \frac{1}{2M_2}(P_4 - P_3). \tag{84}$$

For a finite lattice the last equation has to be solved subject to appropriate boundary conditions.

It is remarkable that the lattice loses its stiffness along the M_2 -diagonals which coincide with the characteristics of the hyperbolic operator in (3.6). As we have already mentioned this results in a slow light phenomenon. We also note that the lattice governed by equation (3.6) demonstrates a similarity with a thin elastic shell of negative Gaussian curvature described by hyperbolic equations (e.g. (**30**), (**31**)).

To summarise, the asymptotic behaviour of this discrete system in two-dimensions is completely characterised by continuum PDEs, valid in the neighbourhood of the standing wave frequencies, that build in the micro-mechanics. In the special case of an infinite, perfect, lattice one can adopt the quasi-periodic Bloch condition and cross-validate the behaviour deduced from the PDEs with the dispersion relations for the lattice. The asymptotics are remarkably accurate almost completely covering the dispersion diagram shown in figure 7.

4. Concluding remarks

The asymptotic theory for lattice structures presented here allows for many generalisations to, say, three dimensions, for localisation in two- or three-dimensions or to engineering structures all of which will rely on understanding the behaviour of an elementary lattice cell. In particular, many engineering structures consist of regular frames and in the case of a discrete network of continuous strings (e.g. see (**32**)) this results in an infinite number of standing modes which can be treated separately; the high frequency homogenization technique can again be applied. In the frame structures there are several situations where

dispersion curves become very close, or even cross, and even in those cases the asymptotic technique still captures the behaviour.

On the cell, the masses oscillate perfectly in-phase or out-phase etc, so we can generate an effective, homogenized, equation of the macroscale that has this behaviour in-built. This effective equation can then be solved entirely on the macro-scale and gives a continuum equation that has the micro-structural behaviour implicit. The localisation phenomena that we highlight in section 2.6 clearly demonstrate this.

The square lattice, chosen as our example for two-dimensional lattices, has considerable geometrical and physical symmetries. These lead to multiple eigenvalues occurring in some cases and, for the infinite perfect lattice, the local behaviour for the Bloch problem (illustrated in figure 7) is remarkably rich. In terms of spectral theory it is quite remarkable the diversity of partial differential eigenvalue problems that emerge, these range from decoupled second order PDEs (3.5,3.3), coupled first order PDEs (3.4,3.4) that then degenerate requiring a higher order correction (3.4), and even fourth order PDEs (3.3). For the Bloch problem the local dependence of frequency on wavenumber that emerges directly from the continuum PDEs is either linear, quadratic, quartic or flat, illustrating a wide variety of asymptotic behaviour, all of which comes naturally from the two-scales approach that we adopt. We note that the differential matrix, and two-scales, approach that we use is not specific, or limited, to the square lattice geometry and other lattice geometries formed by hexagons or triangles can be treated using this formalism.

In passing we have noted that the differential eigenvalue problems, at least for the diatomic chain lattice, equations (2.4), (2.5), are mathematically identical to those from the asymptotic theory of high frequency long-waves in acoustic and elastic waveguides (**21**, **22**, **23**, **24**). For the long-wave high frequency behaviour in acoustic or elastic waveguides the wave itself is very close to the cut-off frequency and is almost in transverse thickness resonance; thus, although the frequency may be high, the wavelength remains very long. For the lattice structure, the standing waves are playing the role of the transverse thickness resonance in the waveguide. Across the elementary cell the standing waves can occur at high frequencies and if we consider the phase shift from one cell to another this varies slowly and if we define a Bloch wavelength relative to the Bloch wavenumber then it is long even though the frequency is high. Thus one can draw parallels between these two, apparently quite different, physical situations.

The analysis of localization phenomena for lattices is also similar to that occurring in the high frequency long-wave waveguide theory. Localization is possible in waveguides due to variation in guide curvature, thickness, material properties or nonlinear effects. In the latter case, we can therefore draw on the analogy for discrete lattices and anticipate that extra effects such as weak nonlinearity in the strings will lead to localization in a similar manner to that employed by (**33**) for nonlinearity in elastic waveguides.

The two-scales asymptotic approach, in conjunction with building in the standing wave behaviour on the elementary lattice cell, breaks free from the usual long-wave low-frequency homogenization approach and enables us to move to high frequencies. We anticipate that this approach, also valid in continuous periodic systems with a mismatch in scales (**17**), will allow us to investigate and model micro-mechanical systems on the macroscale in parameter regimes previously inaccessible.

Acknowledgements

RVC thanks NSERC (Canada) for support through the Discovery Grant Scheme. JK thanks the University of Alberta for its hospitality and support, during the period whilst this research was carried out, under the Visiting Scholar program. Support from the EPSRC (UK) under grant EP/H021302 is also gratefully acknowledged.

References

1. C. Kittel, Introduction to solid state physics, 7th Edition, John Wiley & Sons, New York, 1996.
2. L. Brillouin, Wave propagation in periodic structures: electric filters and crystal lattices, 2nd Edition, Dover, New York, 1953.
3. L. J. Gibson, M. F. Ashby, Cellular solids: structures and properties, 2nd Edition, Cambridge University Press, Cambridge, 1997.
4. P. G. Martinsson, A. B. Movchan, Vibrations of lattice structures and phononic band gaps, *Q. Jl. Mech. Appl. Math.*, **56** (2003) 45–64.
5. J. S. Jensen, Phononic band gaps and vibrations in one- and two-dimensional mass-spring structures, *J. Sound Vib.* **266** (2003) 1053–1078.
6. J. D. Joannopoulos, S. G. Johnson, J. N. Winn, R. D. Meade, Photonic Crystals, Molding the Flow of Light, 2nd Edition, Princeton University Press, Princeton, 2008.
7. E. Yablonovitch, Photonic crystals: semiconductors of light, *Scientific American* **285** (2001) 34–41.
8. F. Zolla, G. Renversez, A. Nicolet, B. Kuhlmey, S. Guenneau, D. Felbacq, Foundations of photonic crystal fibres, Imperial College Press, London, 2005.
9. A. B. Movchan, N. V. Movchan, C. G. Poulton, Asymptotic Models of Fields in Dilute and Densely Packed Composites, ICP Press, London, 2002.
10. S. D. M. Adams, R. V. Craster, S. Guenneau, Bloch waves in periodic multi-layered waveguides, *Proc. R. Soc. Lond.* A **464** (2008) 2669–2692.
11. A. S. Phani, J. Woodhouse, N. A. Fleck, Wave propagation in two-dimensional periodic lattices, *J. Acoust. Soc. Am.* **119** (2006) 1995–2005.
12. A. A. Maradudin, Some effects of point defects on the vibrations of crystal lattices, *Rep. Prog. Phys.* **28** (1965) 332380.
13. A. B. Movchan, L. I. Slepyan, Band gap Green functions and localised oscillations, *Proc. R. Soc. Lond.* A **463** (2007) 2709–2727.
14. K. B. Dossou, L. C. Botten, R. C. McPhedran, A. A. A. abd C. Martijn de Sterke, Gap-edge asymptotics of defect modes in two-dimensional photonic crystals, *Optics Express* **15** (2007) 4753–4762.
15. S. Mahmoodian, R. C. McPhedran, C. Martijn de Sterke, K. B. Dossou, C. G. Poulton, L. C. Botten, Single and coupled degenerate defect modes in two-dimensional photonic crystal band gaps, *Phys. Rev. A* **79** (2009) 013814.
16. P. A. Martin, Discrete scattering theory: Green's function for a square lattice, *Wave Motion* **43** (2006) 619–629.
17. R. V. Craster, J. Kaplunov, A. V. Pichugin, High frequency homogenization for periodic media, to appear *Proc R Soc Lond A* http://dx.doi.org/10.1098/rspa.2009.0612.
18. V. L. Berdichevski, Variational principles of continuum mechanics, Nauka, Moscow, 1983, in Russian.

19. J. D. Kaplunov, L. Yu. Kossovich, E. V. Nolde, Dynamics of Thin Walled Elastic Bodies, Academic Press, New York, 1998.
20. K. C. Le, Vibrations of shells and rods, Springer, Berlin, 1999.
21. D. Gridin, R. V. Craster, A. T. I. Adamou, Trapped modes in curved elastic plates, *Proc R Soc Lond A* **461** (2005) 1181–1197.
22. J. D. Kaplunov, G. A. Rogerson, P. E. Tovstik, Localized vibration in elastic structures with slowly varying thickness, *Quart. J. Mech. Appl. Math.* **58** (2005) 645–664.
23. D. Gridin, A. T. I. Adamou, R. V. Craster, Electronic eigenstates in quantum rings: Asymptotics and numerics, *Phys Rev B* **69** (2004) 155317.
24. J. Postnova, R. V. Craster, Trapped modes in elastic plates, ocean and quantum waveguides, *Wave Motion* **45** (2008) 565–579.
25. L. Infeld, T. E. Hull, The factorization method, *Rev. Modern Phys.* **23** (1951) 21–68.
26. V. V. Zalipaev, A. B. Movchan, I. S. Jones, Waves in lattices with imperfect junctions and localized defect modes, *Proc. R. Soc. Lond.* A **464** (2008) 2037–2054.
27. R. V. Craster, S. Guenneau, S. D. M. Adams, Mechanism for slow waves near cutoff frequencies in periodic waveguides, *Phys. Rev. B* **79** (2009) 045129.
28. J. Kaplunov, E. Nolde, G. A. Rogerson, An asymptotic analysis of initial-value problems for thin elastic plates, *Proc. R. Soc. Lond.* A **462** (2006) 2541–2561.
29. E. Nolde, Qualitative analysis of initial-value problems for a thin elastic strip, *IMA J. Appl. Math* **72** (2007) 348–375.
30. A. L. Goldenveizer, Theory of elastic thin shells, Pergamon Press, Oxford, London, New York, Paris, 1961, transl. from Goldenveizer, A. L. (1953) *Teoriia uprugykh tonkikh obolochek,* Moscow: Gostekhteoretizdat. In Russian.
31. D. Caillerie, A. Raoult, E. Sanchez-Palencia, On internal and boundary layers with unbounded energy in thin shell theory. hyperbolic characteristic and non-characteristic cases, *Asymptotic Analysis* **46** (2006) 189–220.
32. E. Nolde, R. V. Craster, J. Kaplunov, Dynamic high frequency homogenization for periodic nets, under review (2010).
33. J. Kaplunov, E. Nolde, An example of a quasi-trapped mode in a weakly non-linear elastic waveguide, *Comptes Rendus Mecanique* **336** (2008) 553–558.